Available online at www.sciencedirect.com

ScienceDirect

www.elsevier.com/locate/jes

JES JOURNAL OF ENVIRONMENTAL SCIENCES

www.jesc.ac.cn

Pollution levels, composition characteristics and sources of atmospheric $PM_{2.5}$ in a rural area of the North China Plain during winter

Xiaoxi Zhao[1,2,4,6], *Xiujuan Zhao*[2,*], *Pengfei Liu*[1,3,4,6], *Can Ye*[1,4], *Chaoyang Xue*[1,4], *Chenglong Zhang*[1,3,4], *Yuanyuan Zhang*[1,3,4], *Chengtang Liu*[1,3,4], *Junfeng Liu*[1,3,4], *Hui Chen*[5], *Jianmin Chen*[5], *Yujing Mu*[1,3,4,*]

[1] *Research Center for Eco-Environmental Sciences, Chinese Academy of Sciences, Beijing 100085, China*
[2] *Institute of Urban Meteorology, Chinese Meteorological Administration, Beijing 100089, China*
[3] *Center for Excellence in Urban Atmospheric Environment, Institute of Urban Environment, Chinese Academy of Sciences, Xiamen 361021, China*
[4] *University of Chinese Academy of Sciences, Beijing 100049, China*
[5] *Shanghai Key Laboratory of Atmospheric Particle Pollution and Prevention, Department of Environmental Science and Engineering, Fudan University, Shanghai 200433, China*
[6] *Key Laboratory of Atmospheric Chemistry, China Meteorological Administration, Beijing 100081, China*

ARTICLE INFO

Article history:
Received 27 September 2019
Revised 24 March 2020
Accepted 25 March 2020
Available online 4 May 2020

Keywords:
Rural area
$PM_{2.5}$
Composition
Residential coal combustion
Source apportionment

ABSTRACT

The pollution levels, composition characteristics and sources of atmospheric $PM_{2.5}$ were investigated based on field measurement at a rural site in the North China Plain (NCP) from pre-heating period to heating period in winter of 2017. The hourly average concentrations of $PM_{2.5}$ frequently exceeded 150 μg/m^3 and even achieved 400 μg/m^3, indicating that the $PM_{2.5}$ pollution was still very serious despite the implementation of stricter control measures in the rural area. Compared with the pre-heating period, the mean concentrations of organic carbon (OC), element carbon (EC) and chlorine ion (Cl^-) during the heating period increased by 20.8%, 36.6% and 38.8%, accompanying with increments of their proportions in $PM_{2.5}$ from 37.5%, 9.8% and 5.5% to 42.9%, 12.7% and 7.2%, respectively. The significant increase of both their concentrations and proportions during the heating period was mainly ascribed to the residential coal combustion. The proportions of sulfate, nitrate and ammonium respectively increased from 9.9%, 10.9% and 9.0% in nighttime to 13.8%, 16.2% and 11.1% in daytime, implying that the daytime photochemical reactions made remarkable contributions to the secondary inorganic aerosols. The simulation results from WRF-Chem revealed that the emission of residential coal combustion in the rural area was underestimated by the current emission inventory. Six sources identified by positive matrix factorization (PMF) based on the measurement were residential coal combustion, secondary formation of inorganic aerosols, biomass burning, vehicle emission and raising dust, contributing to atmospheric $PM_{2.5}$ of 40.5%, 21.2%, 16.4%, 10.8%, 8.6% and 2.5%, respectively.

* Corresponding authors:
E-mails: xjzhao@ium.cn (X. Zhao), yjmu@rcees.ac.cn (Y. Mu).

https://doi.org/10.1016/j.jes.2020.03.053
1001-0742/

Introduction

In recent years, the North China Plain (NCP) is undergoing severe haze pollution, which is mainly attributed to the high level of fine particulate matter with diameter less than 2.5 μm ($PM_{2.5}$) (Huang et al., 2014; Wang et al., 2016a; Zhang et al., 2015). For example, the annual mean mass concentration of $PM_{2.5}$ was 102 μg/m^3 in 2013 and 93 μg/m^3 in 2014 in the Beijing-Tianjin-Hebei (BTH) region located in the north of the NCP, which were beyond the national secondary class standard for the daily average limit of 75 μg/m^3 (GB 3095-2012); The days with atmospheric $PM_{2.5}$ concentration exceeded the secondary standard in BTH accounted for nearly half (48%) of the total days in 2015 (Zhang et al., 2017); The hourly $PM_{2.5}$ concentration in southern Hebei even surpassed 900 μg/m^3 in both winters of 2015 and 2016 (Li et al., 2017). Exposure to $PM_{2.5}$ is harmful to human health, resulting in respiratory illnesses, cardiovascular diseases and even premature death (Armbrust et al., 2016; Watson, 2011). Additionally, high level of $PM_{2.5}$ severely reduced visibility (Jiang et al., 2018), resulting in delay of flight, high way and high-speed rail etc. Therefore, the serious $PM_{2.5}$ pollution in the NCP has been aroused great attention by the central and local governments as well as citizens.

Focusing on the serious $PM_{2.5}$ pollution, a series of control measures have been implemented in the NCP for improving the regional air quality since 2010, e.g., the implementation of stricter emission standards for the power, transport and industry sectors (Sheehan et al., 2014). As the consequence, the annual average $PM_{2.5}$ concentrations reduced by 28%-40% from 2013 to 2017 in the BTH region (China Daily, 2018). Based on field measurements (Liu et al., 2017c) and model simulations (Zhang et al., 2017), recent studies further revealed that the residential coal combustion in winter for heating was an important source for $PM_{2.5}$ in the BTH region, and thus the corresponding stricter control measures have also been implemented since 2016, e.g., the residential coal is being quickly replaced by natural gas or electricity for winter heating in most rural areas of the BTH region. However, the effects of the control measures have not been evaluated in the rural areas due to lacking of corresponding field measurements.

In this study, a field campaign was performed at a rural site in the NCP during the wintertime of 2017 to investigate the pollution levels, composition characteristics and sources of atmospheric $PM_{2.5}$ in the rural area. The effect of the current control measures for residential coal combustion was also evaluated through the comparison between the $PM_{2.5}$ levels investigated by this study and our previous studies at the same rural site. Additionally, the weather research and forecasting model coupled with online chemistry (WRF-Chem) model was also adopted for comparably simulating the $PM_{2.5}$ levels between the rural site and Beijing city to reveal the significant influence of residential coal combustion on $PM_{2.5}$ in the rural area.

1. Materials and methods

1.1. Sampling and analysis

The field campaign was conducted from November 1st to December 31st 2017 at the Station of Rural Environment, Research Center for Eco-Environmental Sciences (SRE-RCEES, 38.67°N, 115.25°E) which is situated in an open agricultural field of Dongbaituo (DBT) village, Wangdu county, Baoding, Hebei Province of China. The SRE-RCEES is far away from the sources of industry and power plants. A high way is located to the north of the SRE-RCEES, with direct distance of about 1 km. Detailed information about the SRE-RCEES had been presented in our previous studies (Liu et al., 2016, 2017b, 2017c; Ye et al., 2018).

The concentrations of CO, SO_2, NO_x (NO and NO_2) and $PM_{2.5}$ were measured by using in-situ monitors (43i, 48i, 42i and 1405a TEOM, Thermo-Fisher Scientific, USA) with the detection limits of 0.04 ppmV, 0.12 ppbV, 0.40 ppbV and less than 0.1 μg/m^3, respectively. It should be mentioned that the atmospheric $PM_{2.5}$ mass concentration measured by the 1405a TEOM is usually underestimated because the volatile components (e.g. NH_4NO_3) in $PM_{2.5}$ are easily vaporized on the TEOM filter which is recommended to be kept at 50°C (Weijers et al., 2000). The concentration of ammonia was measured by using differential optical absorption spectroscopy (DOAS), with the detection limits of 1 ppbV. The organic carbon (OC) and element carbon (EC) were measured by using organic/elemental carbon analyzer (TR20N9, CECEP Talroad Technology Co., Ltd., China) with the interagency monitoring of protected visual environments (IMPROVE) thermal-optical reflectance (TOR) protocol with the detection limits of less than 0.5 μg carbon (C)/m^3. The trace elements (Si, Ti, Mn, Fe, Cu, Zn, Se and Pb) of atmospheric $PM_{2.5}$ were measured by using automatic multi-metals monitor (Xact-625, Cooper Environmental Services, USA) with detection limits of less than 0.1 ng/m^3. To make sure the data quality, all above instruments were calibrated every 3 days during the sampling period. The filter samples of atmospheric $PM_{2.5}$ were collected by a programmed multipath (12 channels) $PM_{2.5}$ sampler (2201A, Jectec Science and Technology (Beijing) Co., Ltd., China) on quartz fibre filters (90 mm, Munktell) under medium flow rate of 100 L/min. The duration for collecting each $PM_{2.5}$ filter sample was 2 hours and the filter samples after sampling were put into the dishes-like containers (90 mm, Millipore) and stored in a refrigerator (-20°C) until analysis.

A quarter of each filter sample was extracted ultrasonically with 10 mL of ultrapure water for half an hour. The solution was percolated through a microporous membrane (pore size 0.45 μm; diameter 13 mm), and the water-soluble ions (WSIs) (Cl^-, NO_3^-, SO_4^{2-}, NH_4^+, Mg^{2+}, Ca^{2+} and K^+) in the filtrate were analyzed by ion chromatography (IC6200, Wayeal, China). An anion column (4 mm × 250 mm, Dionex IonPac AS14, Thermo-Fisher Scientific, USA) was adopted to separate the anions in the filtrate through eluent (3.5 mmol/L Na_2CO_3 and 1 mmol/L $NaHCO_3$) at a flow rate of 1.2 mL/min under 25°C. A cation column (TSKgelSuper IC-CR, 4.6 mm × 15 cm) was used to separate the cations in the filtrate through eluent (2.2 mmol/L methanesulfonic acid (MSA) and 1 mmol/L 18-crown-6) at a flow rate of 0.7 mL/min under 40°C. The relative standard deviation (RSD) of each ion was less than 0.5% with the reproducibility test. The detection limits (signal-noise ratio (S/N) = 3) were less than 0.001 mg/L for the anions and cations.

The meteorological conditions including wind speed (WS), wind direction (WD), relative humidity (RH), temperature and pressure were measured online using automatic meteorological station (M451, Vaisala, Finland). The mass concentrations of atmospheric $PM_{2.5}$ in Gucheng (one of national monitoring sites in Beijing city) located in southwest of Beijing were acquired from the website (https://www.aqistudy.cn/) from the Ministry of Environmental Protection of the People's Republic of China and the meteorological conditions in Beijing were collected from the China Meteorological Administration.

1.2. WRF-Chem model

The Weather Research and Forecasting (WRF) model coupled with online chemistry (WRF-Chem) version 4.0.3 (Fast et al., 2006; Grell et al., 2005) was adopted to simulate emission, formation, transformation and transport processes of pollutants. The simulation period spanned from November 1st to

December 31st, 2017. The simulation domain was comprised of 223 × 202 grid cells with 9 km resolution and was centered on the BTH region (39.5°N, 114.8°E). In the vertical dimension, 30 vertical layers were set from the surface (~20 m) to the 50 hPa level, and 12 layers of which were set below 1500 m to resolve the process of planetary boundary layer (PBL). The physics parameterization schemes used in this study included single-layer urban canopy model (UCM) (Kusaka and Kimura, 2004), Noah land-surface (Fei and Dudhia, 2001), Yonsei University planetary boundary layer (YSU PBL) (Hong et al., 2005), Grell-Devenyi ensemble convection (Grell and Dévényi, 2002), Thompson microphysics (Thompson et al., 2008), rapid and accurate radiative transfer mode (RRTM) longwave radiation (Mlawer et al., 1997) and Goddard shortwave radiation (Chou and Suarez, 1994). For the chemistry simulation, the carbon bond mechanism version Z (CBMZ) (Zaveri and Peters, 1999) was used as the gas-phase chemistry module and the model for simulating aerosol interactions and chemistry (MOSAIC) with 8 aerosol diameter bins (Zaveri et al., 2008) was used as the aerosol module. The Fast-J photolysis scheme is used for photolytic rate calculations (Masson, 2000; Wild et al., 2000). The multi-resolution emission inventory for China of 2016 (MEIC-2016) (Li et al., 2014; Liu et al., 2015; Zhang et al., 2009; Zheng et al., 2014) with a resolution of 0.1° × 0.1° (http://www.meicmodel.org/) was used in this study and interpolated to the 9 km grid cells of the model via a bilinear method. Meteorological lateral boundary conditions (LBCs) and initial conditions (ICs) were obtained through the WRF Preprocessing System (WPS), via output from the rapid refresh multiscale analysis and prediction system-short term model (RMAPS-ST), which is an operational model of the institute of urban meteorology (IUM). The RMAPS-ST performed an advanced research version of WRF and WRF data assimilation (WRFDA), and it can provide more accurate meteorological condition to WRF-Chem due to the assimilation of regional and local meteorological data (Liang et al., 2016). Chemical LBCs and ICs are based on prescribed idealized profiles. The simulation started on October 23rd and the first 7 days were treated as spin-up period to allow the pollutants accumulated.

Additionally, the mean bias (MB), root mean square error (RMSE) and index of agreement (IOA), which are usually used to evaluate the performance of simulation results, were calculated by Eqs. (1)-(3), respectively.

$$\mathrm{MB} = \frac{1}{n}\sum_{i=1}^{n}(p_i - o_i) \tag{1}$$

$$\mathrm{RMSE} = \sqrt{\frac{1}{n}\sum_{i=1}^{n}(p_i - o_i)^2} \tag{2}$$

$$\mathrm{IOA} = 1 - \frac{\sum_{i=1}^{n}(p_i - o_i)^2}{\sum_{i=1}^{n}\left(\left(|p_i - O|\right) + \left(|o_i - O|\right)\right)^2} \tag{3}$$

where p_i is the simulation data, o_i is the observation data, and O is the average of observation data.

1.3. *Positive matrix factor (PMF) model*

The receptor model of positive matrix factor (PMF) (Paatero and Tapper, 2010) was applied to identify the $PM_{2.5}$ sources. PMF is a multivariate factor analysis tool that decomposes a matrix of speciated sample data into two matrices-factor contributions and factor profiles that can be interpreted by an analyst as to what sources are represented based on observations at a receptor site (Banerjee et al., 2015; Park et al., 2019; Yu et al., 2019). The Q value which is calculated with the uncertainties of each observation data, can be used to review the distribution for each species to evaluate the stability of the solution. The equation of Q value is listed in Eq. (4), in which u_{ij} is the uncertainty estimate of source j measured in sample i, x_{ij} is the jth species concentration measured in the ith sample, g_{ik} is the species contribution of the kth source to the ith sample, f_{kj} is the jth species fraction from the kth source, and p is the total number of independent sources.

$$Q = \sum_{i=1}^{m}\sum_{j}^{n}\left(\frac{x_{ij} - \sum_{k=1}^{p} g_{ik} f_{ik}}{u_{ij}}\right)^2 \tag{4}$$

Followed the suggestions for PMF analysis by Reff et al. (2012), the PMF was applied in three steps. The first step was preparing the observation data using to be modeled and replacing the poorly or missing data following the methods concluded by Reff et al. (2012), the second step was processing the data with PMF to develop a feasible and robust solution with Q value test, the Q value of best solution was almost equal to the total number of samples times the total number of species used in PMF, the third step was interpreting the solutions according to the previous studies.

2. Results and discussion

2.1. *Pollution levels of atmospheric pollutants in the rural area*

Time series of various atmospheric pollutants in both particle-phase and gas-phase as well as the key meteorological parameters are illustrated in Fig. 1 and their statistical mean concentrations during heating and pre-heating periods are listed in Table 1. Obviously, the $PM_{2.5}$ pollution in the rural area was very serious, e.g., its hourly average concentration frequently exceeded 150 μg/m^3 with the maximal value approaching 380 μg/m^3 during the heating period. The atmospheric concentrations of $PM_{2.5}$ and its major components (OC, EC, Cl^-, NO_3^-, SO_4^{2-} and NH_4^+) as well as the key gas-phase species (CO, SO_2, NH_3, NO_x) remarkably fluctuated during the measurement period, with appearance of pollution episodes marked by relatively high levels of the pollutants usually in 3-4 days. The fluctuations of the pollutants reversely corresponded to the variations of WS, confirming that the WS played a pivotal role in dispersion or accumulation of the pollutants (Zhao et al., 2013). Although the mean WS was faster by 19.2% during the heating period than the pre-heating period (Table 1), the mean concentrations of $PM_{2.5}$, OC, EC, Cl^- as well as CO and SO_2 during the heating period increased by 79.1%, 20.8%, 36.6%, 38.8%, 110.6% and 94.4%, respectively. The remarkable increments of the pollutants were mainly ascribed to strong emissions of the pollutants from additional sources during the heating period, e.g., residential coal combustion is prevailingly adopted for heating during winter in the rural area. The residential coal combustion has been verified to be one of the dominant sources for atmospheric $PM_{2.5}$, OC, EC, Cl^-, CO and SO_2 in the rural area even the whole regions of Beijing-Tianjin-Hebei (BTH) during winter seasons (Liu et al., 2017c). In contrast to the above pollutants, SO_4^{2-} only increased by 10.1% and NH_4^+ by 3.0%, whereas NO_3^- remarkably decreased by 40.3% during the heating period in comparison with the pre-heating period. Atmospheric SO_4^{2-}, NO_3^-, and NH_4^+ are usually called secondary inorganic aerosols (SIA) because they are mainly from the secondary formation through atmospheric photochemical processes (Chan and Yao, 2008; Quan et al., 2015; Tao et al., 2018; Tian et al., 2019; Zhang et al., 2015). The increasing percent of SO_2 concentration was about a factor of 9.4 greater than that of SO_4^{2-} concentration from pre-heating period to

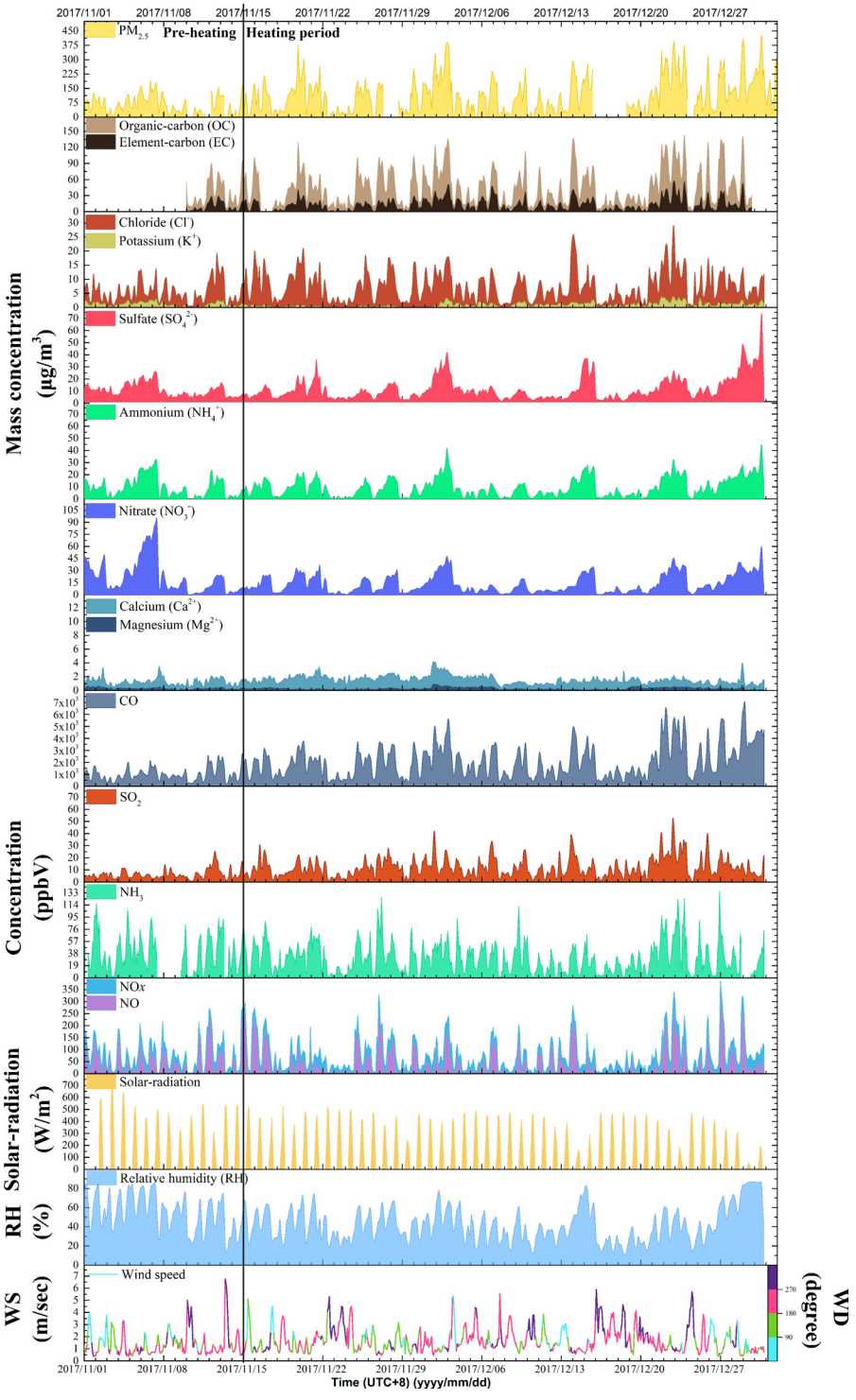

Fig. 1 – Time series of the typical species (OC, EC, Cl^-, NO_3^-, SO_4^{2-} and NH_4^+) in $PM_{2.5}$, key gas species (CO, SO_2, NH_3 and NO_x) and meteorological factors (solar radiation, RH (relative humidity), WS (wind speed) and WD (wind direction)) during winter in Dongbaituo (DBT) rural area. Wind direction: 0 and 360 is north, 90 is east, 180 is south and 270 is west; UTC: coordinated universal time.

the heating period, indicating that SO_4^{2-} formation through oxidation of SO_2 by the major atmospheric photo-oxidants (OH radicals and H_2O_2 etc.) might be greatly suppressed due to relatively low photochemical reactivity under the conditions of low temperature and weak sunlight intensity during the heating period. The remarkably decrease of NO_3^- during the heating period could further verify the relatively low photochemical reactivity because its precursors (NO_x) were almost identical between heating and pre-heating periods. Evident ammonia (NH_3) emission from the residential coal combustion has been reported by a previous study (Li et al., 2016), but atmospheric concentration of NH_3 measured was about 20.6% lower during the heating period than during the pre-heating period. The relatively low air temperature during the heating

Table 1 – Comparison of the mean concentrations of $PM_{2.5}$ components between the pre-heating period and the heating period at the sampling site of Dongbaituo village (DBT) (Mean ± SD).

	Total $PM_{2.5}$ ($\mu g/m^3$)	SO_4^{2-} ($\mu g/m^3$)	NO_3^- ($\mu g/m^3$)	NH_4^+ ($\mu g/m^3$)	Cl^- ($\mu g/m^3$)	K^+ ($\mu g/m^3$)	Mg^{2+} ($\mu g/m^3$)	Ca^{2+} ($\mu g/m^3$)	OC ($\mu g/m^3$)	EC ($\mu g/m^3$)
Pre-heating	63.9 ± 46.4	11.2 ± 5.4	23.7 ± 14.1	10.3 ± 8.5	Cl^-5.5 ± 4.0	1.2 ± 0.8	0.3 ± 0.1	1.29 ± 0.6	38.0 ± 33.9	10.0 ± 9.0
Heating	114.4 ± 92.9	12.3 ± 10.0	14.1 ± 12.0	10.6 ± 8.5	7.7 ± 5.6	1.0 ± 0.7	0.3 ± 0.2	1.63 ± 0.6	45.9 ± 36.3	13.6 ± 12.5
Ratio of increment	79.1%	10.1%	−40.3%	3.0%	38.8%	−17.6%	0%	26.8%	20.82%	36.6%

	NO_x (ppbV)	NO (ppbV)	SO_2 (ppbV)	NH_3 (ppbV)	CO (ppbV)	Wind speed (m/sec)
Pre-heating	83.8 ± 62.5	56.8 ± 57.4	6.3 ± 4.3	39.0 ± 27.8	1.0 ± 0.6	1.4 ± 1.1
Heating	82.3 ± 73.3	53.1 ± 66.2	12.3 ± 8.6	31.0 ± 24.5	2.1 ± 1.4	1.7 ± 1.0
Ratio of increment	−1.7%	−3.0%	94.4%	−20.6%	110.6%	19.2%

OC: organic carbon; EC: black carbon.

period was in favor of conversion of gas-phase NH_3 into NH_4^+ in particle-phase through partition (Wang et al., 2015), which could be certified by the slight increase of NH_4^+ concentration during the heating period. On the other hand, NH_3 emission from biogenic sources (such as animal waste) would be greatly reduced during the heating periods due to suppression of biogenic activity by the low air temperature (Bleizgys and Balezentiene, 2014). As one of the indicators of biomass burning, the mean concentration of K^+ was about 17.1% lower during the heating period than pre-heating period, implying that biomass burning might be slighter during the heating period (Mason et al., 2016). It should be mentioned that the relatively low mean concentration of K^+ during the heating period was mainly ascribed to the extremely low concentrations during the period of 15th - 30th November, whereas the K^+ concentrations after 30th November were comparable to those during the pre-heating period (Fig. 1). The slight increase of the concentrations of Ca^{2+} during the period from 15th November to 6th December (Fig. 1) were attributed to the relatively low RH and high WS which are in favor of raising dust (Zhao et al., 2013), resulting in the mean concentration of Ca^{2+} increasing by 17.1% during the heating period.

Focusing on the serious haze pollution during winter, a series of strict control measures have been implemented in the rural areas of BTH, for example, residential coal combustion for heating has been replaced by natural gas or electricity in many villages around DBT in 2017, and biomass burning in the field is under stricter supervision in each village. To reveal the effect of the control measures, the levels of $PM_{2.5}$ and its major components obtained in this study are compared with our previous studies at the same sampling site but in different years (Table 2). Compared with the two previous years, the mean concentrations of $PM_{2.5}$ and its major components in winter of 2017 were reduced by about 50%, revealing that the control measures are effective for mitigating the regional pollution of $PM_{2.5}$. Nevertheless, the mean $PM_{2.5}$ concentration in the rural area still largely exceeded the national standards, stricter control measures are urgently needed for further improving the air quality.

Table 2 – Comparison of the mean concentrations of $PM_{2.5}$ components among different years at the sampling site of DBT.

Mean concentration ($\mu g/m^3$)	2017 DBT winter	2015 DBT winter	2014 DBT winter
$PM_{2.5}$	114.4±92.9	218.4±87.1	-
OC	45.9±36.3	100.0±42.9	-
EC	13.6±12.5	21.6±10.2	-
Nitrate	14.1±12.0	21.0±12.2	23.7±24.3
Sulfate	12.3±10.0	24.1±16.1	22.3±20.4
Ammonium	10.6±8.5	18.7±11.7	16.8±13.9
Chloride	7.7±5.6	13.4±6.0	14.0±1.5
Potassium	1.0±0.9	3.1±1.3	2.4±1.5

2.2. *Composition characteristics of $PM_{2.5}$ in the rural area*

To further reveal the contribution of residential coal combustion for heating to atmospheric $PM_{2.5}$, the proportion of each component to the $PM_{2.5}$ was respectively analyzed during the pre-heating period and heating period, which are illustrated in Fig. 2a Compared with the pre-heating period, the proportions of OC, EC and Cl^-, which are the major components of the smoke from residential coal combustion (McCulloch et al., 1999), increased from 37.5% to 42.9%, from 9.8% to 12.7% and from 5.5% to 7.2%, respectively, implying that the residential coal combustion was still an important source for $PM_{2.5}$ in the rural area despite the implementation of strict control measures. In contrast to the significant increase of the proportions for OC, EC and Cl^- during the heating period, the proportion for NO_3^- remarkably decreased from 23.3% to 13.1%, while the SO_4^{2-} proportion only slightly increased from 11.0% to 11.5% and NH_4^+ proportion was almost kept a constant. The slight increase of SO_4^{2-} proportion during the heating period was mainly attributed to the emissions of both SO_4^{2-} and its precursor of SO_2 from residential coal combustion (Dai et al., 2019). Besides the suppression of SIA formation due to the relatively weak photochemical reactivity during the heating period, the variations of the SIA proportions from pre-heating period to the heating period also revealed that the primary emissions of pollutants were the dominant source for atmospheric $PM_{2.5}$.

To qualitatively identify the contribution of photochemical reactions to the SIA, the proportions of the components to $PM_{2.5}$ in daytime and nighttime were respectively analyzed, which are shown in Fig. 2b. It is evident that the proportions of the major components in $PM_{2.5}$ varied significantly from nighttime to daytime, e.g., SO_4^{2-} increased from 9.9% to 13.8%, NO_3^- from 10.9% to 16.2% and NH_4^+ from 9.0% to 11.1%, whereas OC decreased from 46.5% to 37.6% and EC from 14.0% to 10.9%, implying that the daytime photochemical reactions still made remarkable contributions to the SIA under the cold winter condition. Although the daytime photochemical processes can also make contribution to atmospheric secondary organic aerosols (SOA, part of the OC) through photooxidation of volatile organic compounds (VOCs) (Li et al., 2017), the ra-

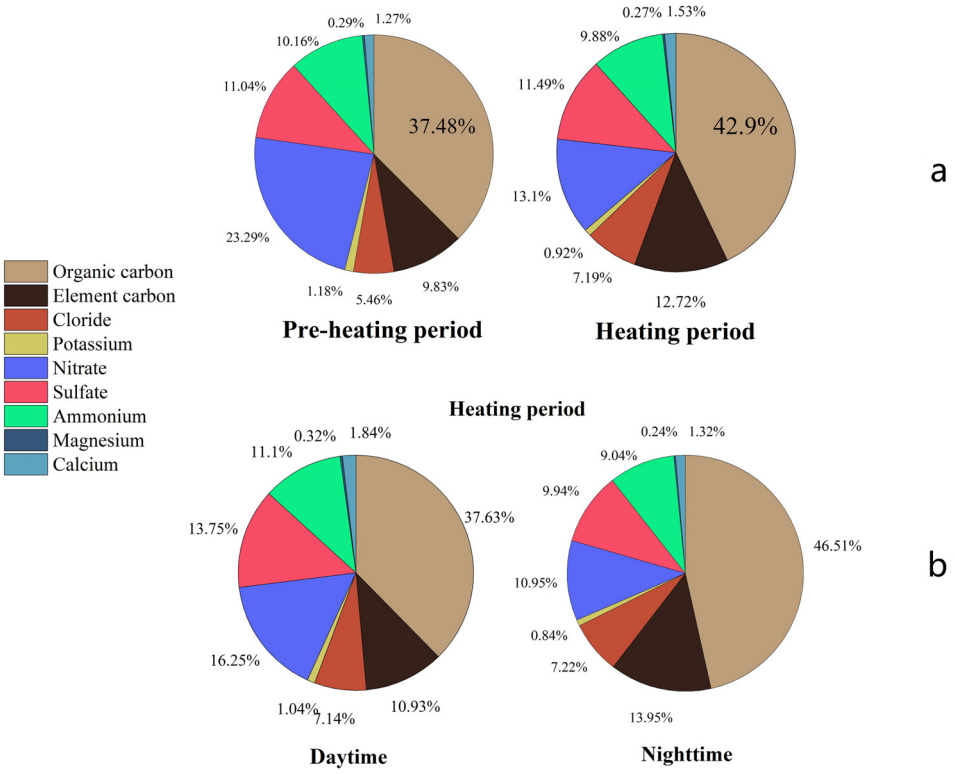

Fig. 2 – Mass proportions of the key species in $PM_{2.5}$ (a) during the pre-heating and heating period and (b) in nighttime and daytime during the heating period at the DBT site.

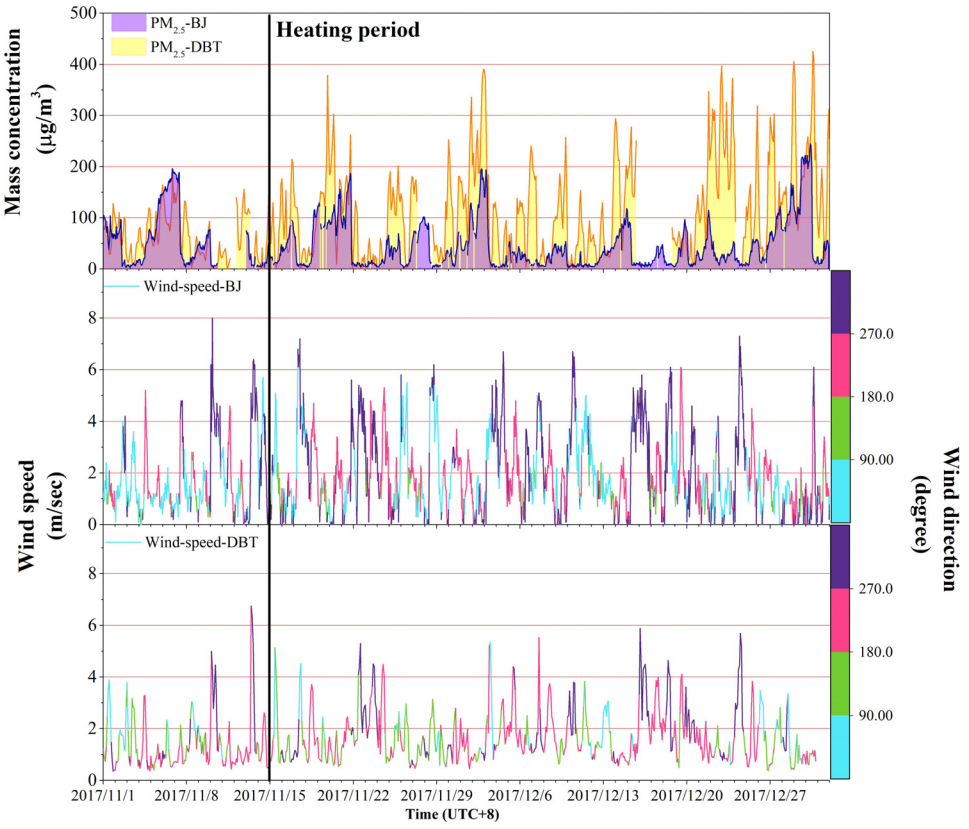

Fig. 3 – Time series of $PM_{2.5}$ mass concentration, WS and WD in DBT rural area and BJ (Beijing) urban area.

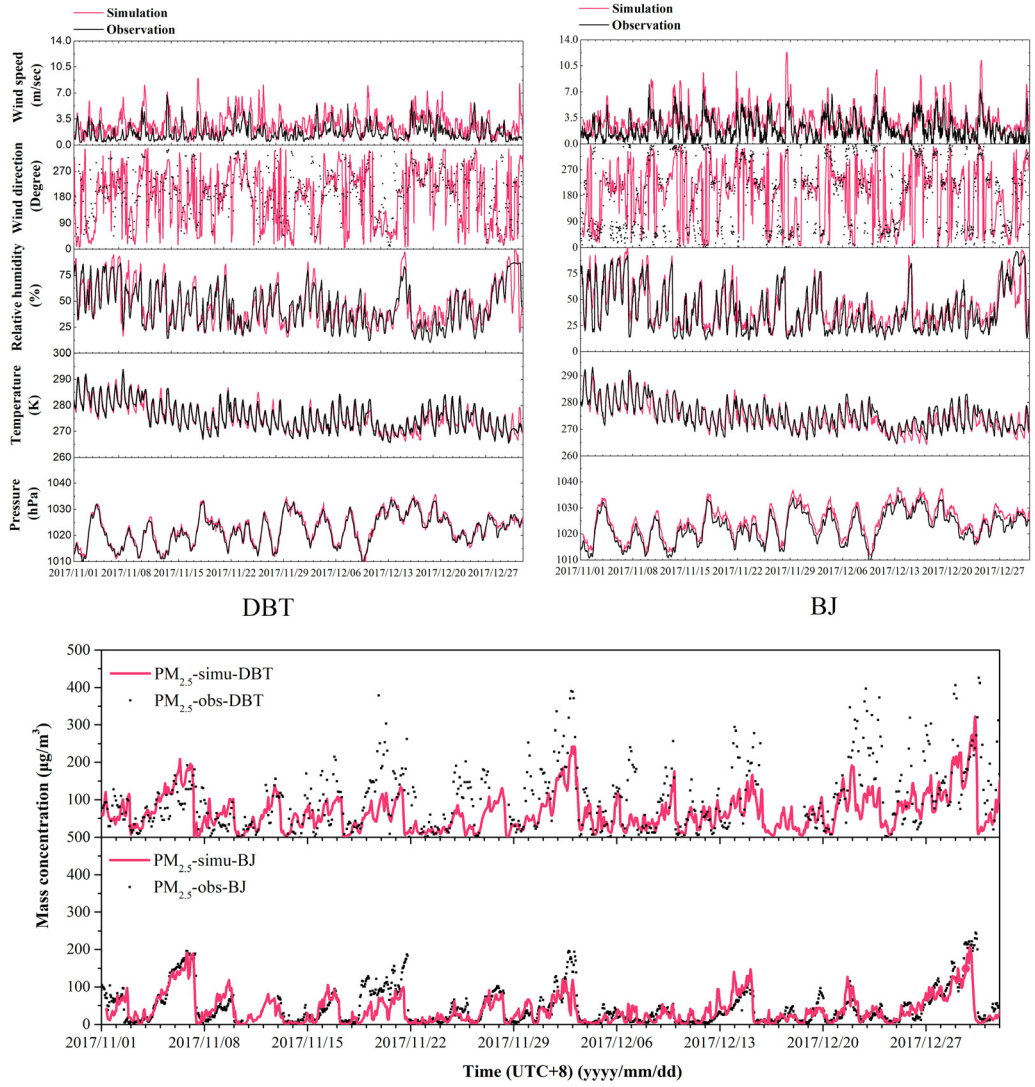

Fig. 4 – Time series of $PM_{2.5}$ and meteorological conditions simulation and observation in DBT and BJ.

tio of OC to EC only slightly increased from 3.32 in nighttime to 3.45 in daytime, indicating that the atmospheric OC at the rural site was dominated by the primary emission from residential coal combustion.

In contrast to the remarkable reduction of the proportions of OC and EC in daytime, the proportion of Cl^- was almost kept constant in both daytime and nighttime. Therefore, the daytime photochemical reactions were suspected to make evident contribution to the water-soluble Cl^- besides the direct emission from the residential coal combustion, e.g., $ClNO_2$ and Cl_2 formed through the heterogenous reactions in nighttime (Yun et al., 2018) or direct emission from the coal combustion can be easily photolyzed in daytime to Cl atoms which react fast with alkanes to form water-soluble HCl. Unexpectedly high levels (several hundred pptV) of $ClNO_2$, Cl_2 and ClBr were also found by Hong kong polytechnic university during the field campaign at the DBT site, which was suspected to play important role in initiating photochemical reactions.

2.3. *Comparison of $PM_{2.5}$ pollution levels between DBT and Beijing city*

Our previous investigations (Liu et al., 2017c) revealed that the pollution levels of $PM_{2.5}$ in autumn and winter were significantly higher in the rural area of DBT than in Beijing city. Synchro-comparison of $PM_{2.5}$ levels between the DBT and Beijing was further conducted in this study to reveal relative effect of the strict control measures in the rural areas. As shown in Fig. 3, the $PM_{2.5}$ levels at both the sampling sites of DBT and Gucheng (one of national monitoring sites in Beijing city) were approximately same during the pre-heating period, which was in contrast with our previous comparisons about much higher $PM_{2.5}$ concentrations in DBT, indicating the control measures especially for biomass burning might be effective. However, the $PM_{2.5}$ levels at the DBT were still a factor of 2 higher than those at the sampling site of Beijing for almost all pollution episodes during the heating period. Besides the strong emissions of residential coal combustion in DBT, meteorological factors were also suspected to play important role to account for the large difference between DBT and Beijing, e.g., the WS were evidently faster in Beijing than in DBT during the heating period (Fig. 3). The regional emission strengths must evidently increase during the heating period due to additional fossil fuel energy consumption for heating despite the implementation of stricter control measures in the BTH region, whereas the peak levels of $PM_{2.5}$ at the sampling site of Beijing during the pre-heating period were higher than those of the most pollution cases during the heating period. To verify that the reduction of $PM_{2.5}$ in Beijing during

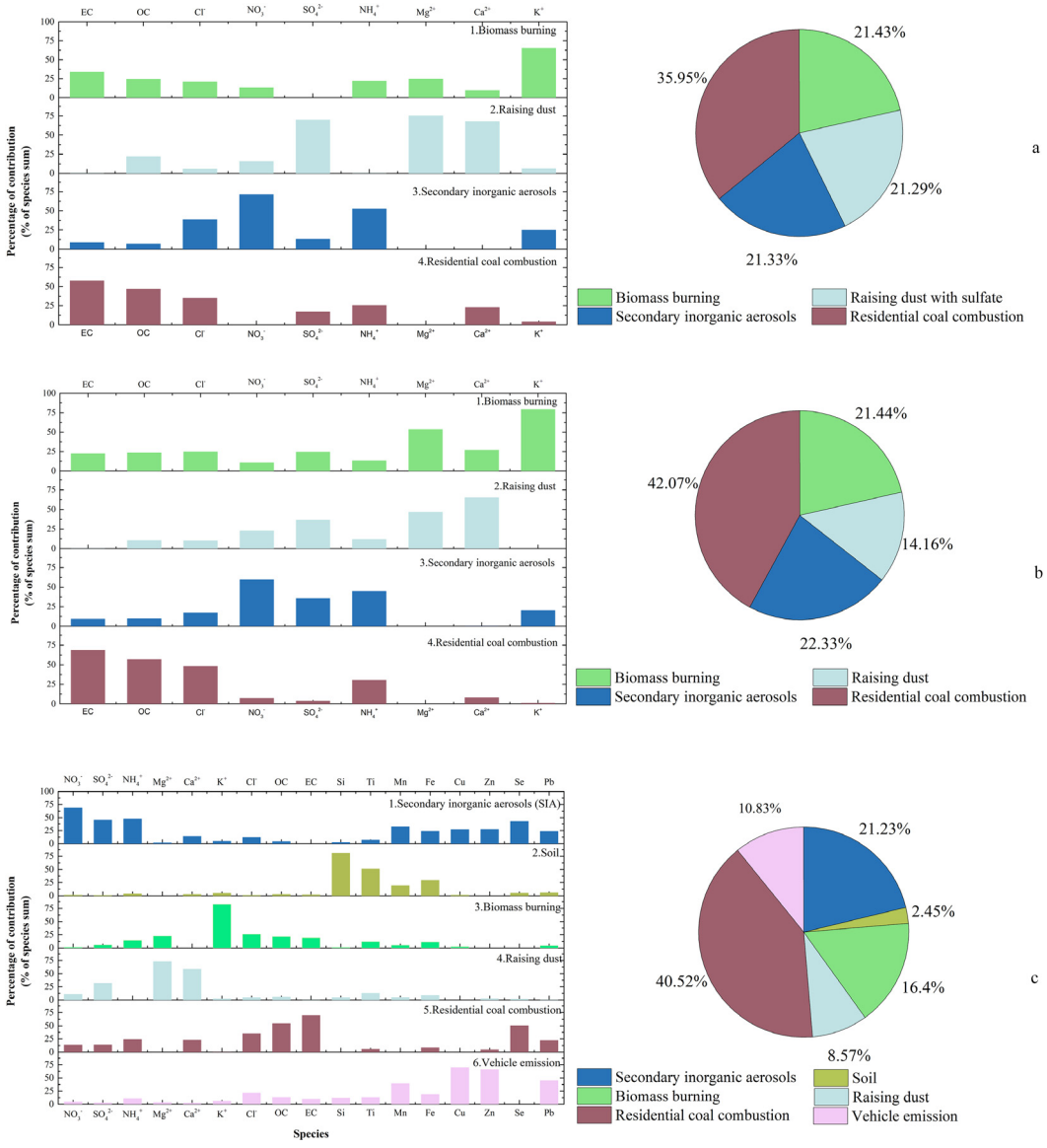

Fig. 5 – Results of PMF (positive matrix factor) analysis with 9 species during (a) pre-heating and (b) heating period in DBT rural area and (c) results of PMF analysis with 17 species during heating period in DBT rural area.

the heating period was ascribed to meteorological factors, a WRF-Chem model was adopted for simulation with input of a fixed inventory (MEIC-2016) during both the pre-heating and the heating periods. The results are shown in Fig. 4 and the statistical parameters of MB, RMSE and IOA are present in Table 3. The WS both in Beijing (measurement at meteorological station of No. 54511, 39.82°N, 116.48°E) and DBT were generally overestimated by the model with the relatively low MB of 1.37 and 1.25 m/sec, the relatively low RMSEs of 1.91 and 2.09 m/sec and the considerable IOA of 0.58 and 0.66 (when IOA is higher, the performance of simulation is better), which were mainly ascribed to the WS measured and simulated were at different heights (e.g., ~5 m for the measurements at DBT and 10 m for the simulation). Whereas the daily variation trends of WS, WD, *T* and RH of the model simulation were in good agreement with the measurements, the MB and RMSE of simulation for *T* and RH in DBT and BJ (Beijing) were relatively low and the IOA of simulation for *T* and RH were relatively high (> 0.9) (Table 3). Thus, the influence of meteorological factors on $PM_{2.5}$ concentration could be distinguished by the model simulation. As expected, the daily variation trends of $PM_{2.5}$ simulated by the model with a considerable IOA of 0.75 in DBT and a relatively high IOA of 0.90 in BJ were well in line with the measurements in both Beijing and DBT (Fig. 4) due to well simulation of the variation trends for meteorological factors by the model. The $PM_{2.5}$ concentrations simulated in DBT during the pre-heating period were comparable to those during the heating period, whereas in Beijing the simulated $PM_{2.5}$ concentrations during the pre-heating period were evidently higher than those during the heating period, confirming that the meteorological factors were more favorable for dispersion of pollutants in Beijing than in DBT during the heating periods. Additionally, the $PM_{2.5}$ concentrations simulated in Beijing were in good agreement with the measurements with a relatively low MB of -3.63 μg/m^3 and a relatively low RMSE of 25.35 μg/m^3 during both pre-heating and heating periods, whereas in DBT the simulated $PM_{2.5}$ concentrations with a larger MB of -35.70 μg/m^3 and a larger RMSE of 75.64 μg/m^3 were significantly lower than the measurements during the heating period, implying that the emission from residential

Table 3 – Performance of model simulation at DBT rural site and BJ urban area.

Site	Statistical parameter	$PM_{2.5}$ (μg/m^3)	Wind speed (m/sec)	T (°C)	RH (%)
DBT	MB	-35.70	1.37	-0.20	0.79
	RMSE	75.64	1.91	1.83	10.83
	IOA	0.75	0.58	0.97	0.92
BJ	MB	-3.63	1.25	-0.66	-3.16
	RMSE	25.35	2.09	2.26	13.82
	IOA	0.90	0.68	0.95	0.84

MB: mean bias; RMSE: root mean squared error; IOA: index of agreement.

coal combustion was largely underestimated in the inventory adopted in the model. Compared with the observation, the simulated $PM_{2.5}$ was underestimated by 47.64 μg/m^3 during the heating period. Based on the source analysis results in Section 2.4, the coal combustion source during the heating period accounted for 40.52%, being equal to 41.9 μg/m^3 which was in line with the underestimation of the simulated $PM_{2.5}$.

2.4. *Source apportionment using PMF in DBT rural area*

The source apportionment was respectively conducted for the pre-heating and heating periods by using the PMF analysis (Sun et al., 2016, 2014, 2004) based on pre-treated observation data including 9 species, 60 samples during pre-heating period and 474 samples during heating period in this study. The results are illustrated in Fig. 5a and b. Obviously, four distinct sources could be identified for both the pre-heating and heating periods with the Q value of 455 and 4668, that are the best results because the Q value was approximately equal to the product of the number of species and the number of samples. The first source was designated to biomass burning based on the dominant species of K^+, Cl^-, OC and EC (Zhang et al., 2019). The second source was attributed to raising dust because it was dominated by Ca^{2+} and Mg^{2+} which are the tracers of raising dust (Yu et al., 2019). It should be mentioned that SO_4^{2-} also accounted for significant percentage in this source especially during the pre-heating period. As lime milk and calcium oxide are widely used as desulfurizers for coal fired power plants, coal fired power plants were also suspected to make certain contribution to this source sector besides raising dust. The third source was designated to be secondary inorganic aerosols which are characterized by SO_4^{2-}, NO_3^-, and NH_4^+. The fourth source was residential coal combustion because of the dominant species of OC, EC and Cl^- which are the typical tracers of coal combustion (Johnson et al., 2006; Kundu et al., 2010). Compared with the pre-heating period, the percentage contribution of residential coal combustion remarkably increased from 35.95% to 42.07%, whereas that of raising dust decreased from 21.29% to 14.16% during the heating period, which were in line with the fact of extensive residential coal combustion for heating and relatively low wind speed during the heating period.

To further estimate the contributions of residential coal combustion and other sources to atmospheric $PM_{2.5}$ during heating period in DBT rural area, the typical source tracers such as OC, EC and trace metal element were also added in the PMF during heating period in this study. As shown in Fig. 5c, the first factor identified as secondary inorganic aerosols (SIA) source had high loads of NO_3^-, SO_4^{2-} and NH_4^+, contributed 21.2% of $PM_{2.5}$ in DBT rural area. The first factor also had distinct load of element Se, indicating that the SIA source in DBT might be mainly ascribed to coal combustion, because element Se is an essential tracer of coal combustion (Eldred, 2012; Thurston et al., 2011; Xie et al., 2006). The second factor identified as soil source had high loads of crustal elements

Table 4 – Comparison of source apportionment results in this study to previous study.

Site	Date	SIA	BB	RCC	TRAN	DUST	Reference
DBT (rural)	November-December, 2017	21.2%	16.4%	40.5%	10.8%	8.6%	This study
DBT (rural)	Winter, 2015	-	-	58%	-	-	Liu et al., 2017c
WD (urban)	Winter, 2015	-	-	43%	-	-	Liu et al., 2017c
BD (urban)	Winter, 2015	-	-	49%	-	-	Liu et al., 2017c
BJ (urban)	Winter, 2015	-	-	32%	-	-	Liu et al., 2017c
BJ (urban)	2001-2004	19%	12%	16%	28%	20%	Zhang et al., 2007
BJ (urban)	2012-2013	48.2%	8.7%	14.1%	12.4%	5.3%	Li et al., 2019
BJ (urban)	2012-2013	48.1%	11.7%	11.1%	24.7%	4.3%	Zíková et al., 2016
LZ (urban)	2014-2015	16.6%	8.0%	22.3%	21.7%	21.8%	Wang et al., 2016c
TJ (urban)	June-August, 2015	26.1%	10.2%	16.5%	25.4%	25.4%	Liu et al., 2017a
TJ (urban)	December 2013 - January 2014	25.5%	4.2%	44.6%	13.1%	12.6%	Wang et al., 2016b
BJ (urban)	2014-2015	40.5%	4.5%	5.6%	24.9%	8.6%	Huang et al., 2017
TJ (urban)	2014-2015	29.2%	5.3%	12.4%	15.2%	11.7%	Huang et al., 2017
SJZ (urban)	2014-2015	36.4%	2.8%	15.5%	17.3%	8.5%	Huang et al., 2017
BJ (urban)	2013-2014	-	-	14.3%-16.1%	19.9%-22.4%	9.2%-10.3%	EPB
TJ (urban)	2013-2014	-	-	17.8%-21.1%	13.2%-15.6%	19.8%-23.4%	EPB
SJZ (urban)	2013-2014	-	-	20.0%-21.9%	10.5%-11.6%	15.8%-17.3%	EPB
BJ (urban)	January, April, July and October in 2014	19.9%	-	24.0%	25.2%	12.9%	Gao et al., 2018
TJ (urban)	January, April, July and October in 2014	13.1%	-	25.6%	23.5%	26.4%	Gao et al., 2018
LF (urban)	January, April, July and October in 2014	4.3%	-	40.7%	12.0%	21.4%	Gao et al., 2018
BD (urban)	January, April, July and October in 2014	9.7%	-	34.8%	14.0%	16.9%	Gao et al., 2018

EPB: Beijing Municipal Environmental Protection Bureau (http://www.bjepb.gov.cn/), Tianjin Municipal Environmental Protection Bureau; BB: biomass burning; SIA: secondary inorganic aerosols; RCC: residential coal combustion; TRAN: vehicle/traffic/transportation emission; DUST: soil/dust sources; BD: Baoding; BJ: Beijing; LZ: Lanzhou; TJ: Tianjin; SJZ: Shijiazhuang; LF: Langfang.

including Si, Ti, Fe and Mn (Park et al., 2019), contributed to $PM_{2.5}$ of 2.5%. The third factor identified as biomass burning source had high loads of K^+, Cl^-, OC and EC (Zhang et al., 2019), contributed to 16.4% of $PM_{2.5}$. The fourth factor identified as raising dust source had high loads of Mg^{2+} and Ca^{2+} which are the tracers of raising dust (Yu et al., 2019), contributed to 8.6% of $PM_{2.5}$. The fifth factor identified as residential coal combustion source had high loads of OC, EC, Cl^- and Se, because all of OC, EC, Cl^- and Se are the typical tracers of coal combustion (Johnson et al., 2006; Kundu et al., 2010). The residential coal combustion source contributed to 40.5% of $PM_{2.5}$ in DBT. The sixth factor identified as vehicle emission source had high loads of Cu, Pb and Zn (Ding et al., 2019), because Zn and Cu are the typical tracers of tire wear (Hjortenkrans et al., 2007) and Pb as well as Zn are known to be emitted from lubricating oil (Belis et al., 2013; Zhou et al., 2012) and oil additives (Ålander et al., 2005). The vehicle emission source contributed to 10.8% of $PM_{2.5}$ in DBT. The contribution of residential coal combustion in DBT rural site during heating period was significantly higher than those in most of urban areas reported by previous studies (Table 4). Besides, the contribution of biomass burning was also higher than those in most of urban areas reported by previous studies, the contribution of secondary inorganic aerosols and transportation was slightly lower than that in most of urban area in previous studies. Compared to the previous studies in the same site, the contribution of residential coal combustion in DBT rural area (40.6%) was less than that in 2015 (58%) (Liu et al., 2017c), confirming that the implementation of strict control measures was effective.

3. Conclusions

Compared with the pre-heating period, the significant increase of the absolute concentrations as well as the proportions of OC, EC and Cl^- in $PM_{2.5}$ during the heating period indicated that residential coal combustion for heating was still the major $PM_{2.5}$ source in the rural area. The proportions of SO_4^{2-}, NO_3^- and NH_4^+ in $PM_{2.5}$ evidently increased with decreasing the proportions of OC and EC from nighttime to daytime, suggesting the daytime photochemical reactions made significant contribution to the secondary inorganic aerosols, rather than secondary organic aerosols. The relatively constant proportion of Cl^- in both daytime and nighttime provided evidence that a fraction of Cl^- in $PM_{2.5}$ was from the photolysis of reactive chlorine species besides the direction emission from residential coal combustion, which might play important role in winter atmospheric chemistry of the rural area.

The levels of $PM_{2.5}$ and its major components at the rural area of DBT were remarkably reduced in the winter of this investigated year in comparison with previous years, implying that the stricter control measures currently implemented in the rural area were effective for mitigating $PM_{2.5}$ pollution. The results of source apportionment based on the measurement data and PMF revealed that residential coal combustion was still the dominant source (~40.5%) for $PM_{2.5}$ in the DBT during the heating period, followed by secondary inorganic aerosols (~21.2%), biomass burning (~16.4%), vehicle emission (~10.8%), raising dust (~8.6%) and soil (~2.5%). Therefore, further reduction of the emission from residential coal combustion is still the most effective control measure for improving the air quality in the rural area.

Declaration of competing interest

The authors declared that they have no conflicts of interest to this work.

We declare that we do not have any commercial or associative interest that represents a conflict of interest in connection with the work submitted.

Acknowledgments

This work was supported by the National Natural Science Foundation of China (Nos. 91544211, 41727805, 41575121, and 21707151), the National research program for Key issues in air pollution control (Nos. DQGG0103, DQGG0209, and DQGG0206), the National Key Research and Development Program of China (Nos. 2016YFC0202200, 2017YFC0209703, and 2017YFF0108301) and Key Laboratory of Atmospheric Chemistry, China Meteorological Administration (No. 2018B03).

REFERENCES

Ålander, T., Antikainen, E., Raunemaa, T., Elonen, E., Rautiola, A., Torkkell, K., 2005. Particle emissions from a small two-stroke engine: Effects of fuel, lubricating oil, and exhaust aftertreatment on particle characteristics. Aerosol Sci. Technol. 39, 151–161.

Armbrust, W., Lelieveld, O.H., Tuinstra, J., Wulffraat, N.M., Bos, G.J., Cappon, J., et al., 2016. Fatigue in patients with juvenile idiopathic arthritis: Relationship to perceived health, physical health, self-efficacy, and participation. Pediatr. Rheumatol. 14, 65.

Banerjee, T., Murari, V., Kumar, M., Raju, M.P., 2015. Source apportionment of airborne particulates through receptor modeling: Indian scenario. Atmos. Res. 164-165, 167–187.

Belis, C.A., Karagulian, F., Larsen, B.R., Hopke, P.K., 2013. Critical review and meta-analysis of ambient particulate matter source apportionment using receptor models in Europe. Atmos. Environ. 69, 94–108.

Bleizgys, R., Balezentiene, L., 2014. Assessments of biogenic gas emission processes in cowsheds. Pol. J. Environ. Stud. 23, 1107–1114.

Chan, C.K., Yao, X., 2008. Air pollution in mega cities in China. Atmos. Environ. 42, 1–42.

China Daily, 2018. realized. Air quality targets set by the Action Plan have been fully realized. China Daily, Beijing, China. Available: http://www.gov.cn/xinwen/2018-02/01/content_5262720.htm. Accessed Feberuary 1, 2018.

Chou, M.D., Suarez, M.J., 1994. An efficient thermal infrared radiation parameterization for use in general circulation models. NASA Tech. Memo. 10, 85.

Dai, Q., Bi, X., Song, W., Li, T., Liu, B., Ding, J., et al., 2019. Residential coal combustion as a source of primary sulfate in Xi'an, China. Atmos. Environ. 196, 66–76.

Ding, X., Qi, J., Meng, X., 2019. Characteristics and sources of organic carbon in coastal and marine atmospheric particulates over East China. Atmos. Res. 228, 281–291.

Eldred, R.A., 2012. Comparison of selenium and sulfur at remote sites. J. Air Waste Manage. Assoc. 47, 204–211.

Fast, J.D., Gustafson, W.I., Easter, R.C., Zaveri, R.A., Barnard, J.C., Chapman, E.G., et al., 2006. Evolution of ozone, particulates, and aerosol direct radiative forcing in the vicinity of Houston using a fully coupled meteorology-chemistry-aerosol model. J. Geophys. Res. 111, D21305.

Fei, C., Dudhia, J., 2001. Coupling an advanced land surface–hydrology model with the Penn State–NCAR MM5 modeling system. Part i: Model implementation and sensitivity. Mon. Weather Rev. 129, 569–585.

Gao, J., Wang, K., Wang, Y., Liu, S., Zhu, C., Hao, J., et al., 2018. Temporal-spatial characteristics and source apportionment of $PM_{2.5}$ as well as its associated chemical species in the Beijing-Tianjin-Hebei region of China. Environ. Pollut. 233, 714–724.

Grell, G.A., Dévényi, D., 2002. A generalized approach to parameterizing convection combining ensemble and data assimilation techniques. Geophys. Res. Lett. 29 (14) 38-1-38-4.

Grell, G.A., Peckham, S.E., Schmitz, R., McKeen, S.A., Frost, G., Skamarock, W.C., et al., 2005. Fully coupled "online" chemistry within the WRF model. Atmos. Environ. 39, 6957–6975.

Hjortenkrans, D.S.T., Bo, G., Bergbäck, Häggerud, A.V., 2007. Metal emissions from brake linings and tires: Case studies of Stockholm. Sweden 1995/1998 and 2005. Environ. Sci. Technol. 41, 5224–5230.

Hong, S.Y., Noh, Y., Dudhia, J., 2005. A new vertical diffusion package with an explicit treatment of entrainment processes. Mon. Weather Rev. 134, 2318–2341.

Huang, R.J., Zhang, Y., Bozzetti, C., Ho, K.F., Cao, J.J., Han, Y., et al., 2014. High secondary aerosol contribution to particulate pollution during haze events in China. Nature 514, 218–222.

Huang, X., Liu, Z., Liu, J., Hu, B., Wen, T., Tang, G., et al., 2017. Chemical characterization and source identification of $PM_{2.5}$ at multiple sites in the Beijing–Tianjin–Hebei region, China. Atmos. Chem. Phys. 17, 12941–12962.

Jiang, N., Li, Q., Su, F., Wang, Q., Yu, X., Kang, P., et al., 2018. Chemical characteristics and source apportionment of $PM_{2.5}$ between heavily polluted days and other days in Zhengzhou, China. J. Environ. Sci. 66, 188–198.
Johnson, K.S., Foy, B.D., Zuberi, B., Molina, L.T., Molina, M.J., Xie, Y., et al., 2006. Aerosol composition and source apportionment in the mexico city metropolitan area with pixe/pesa/stim and multivariate analysis. Atmos. Chem. Phys. Discuss. 6, 4591–4600.
Kundu, S., Kawamura, K., Andreae, T.W., Hoffer, A., Andreae, M.O., 2010. Diurnal variation in the water-soluble inorganic ions, organic carbon and isotopic compositions of total carbon and nitrogen in biomass burning aerosols from the Lba-Smocc Campaign in Rondônia. Brazil. J. Aerosol Sci. 41, 118–133.
Kusaka, H., Kimura, F., 2004. Coupling a single-layer urban canopy model with a simple atmospheric model: Impact on urban heat island simulation for an idealized case. J. Meteorol. Soc. Japan 82, 67–80.
Li, H., Zhang, Q., Zhang, Q., Chen, C., Wang, L., Wei, Z., et al., 2017. Wintertime aerosol chemistry and haze evolution in an extremely polluted city of the north china plain: Significant contribution from coal and biomass combustion. Atmos. Chem. Phys. 17, 4751–4768.
Li, M., Zhang, Q., Streets, D.G., He, K.B., Cheng, Y.F., Emmons, L.K., et al., 2014. Mapping asian anthropogenic emissions of non-methane volatile organic compounds to multiple chemical mechanisms. Atmos. Chem. Phys. 14, 5617–5638.
Li, Q., Jiang, J., Cai, S., Zhou, W., Wang, S., Duan, L., et al., 2016. Gaseous ammonia emissions from coal and biomass combustion in household stoves with different combustion efficiencies. Environ. Sci. Tech. Lett. 3, 98–103.
Li, X., Yang, K., Han, J., Ying, Q., Hopke, P.K., 2019. Sources of humic-like substances (hulis) in $PM_{2.5}$ in beijing: Receptor modeling approach. Sci. Total. Environ. 671, 765–775.
Liang, C.S., Duan, F.K., He, K.B., Ma, Y.L., 2016. Review on recent progress in observations, source identifications and countermeasures of $PM_{2.5}$. Environ. Int. 86, 150–170.
Liu, B., Yang, J., Yuan, J., Wang, J., Dai, Q., Li, T., et al., 2017a. Source apportionment of atmospheric pollutants based on the online data by using PMF and ME2 models at a megacity, China. Atmos. Res. 185, 22–31.
Liu, C., Ma, Z., Mu, Y., Liu, J., Zhang, C., Zhang, Y., et al., 2017b. The levels, variation characteristics, and sources of atmospheric non-methane hydrocarbon compounds during wintertime in Beijing, China. Atmos. Chem. Phys. 17, 10633–10649.
Liu, F., Zhang, Q., Tong, D., Zheng, B., Li, M., Huo, H., et al., 2015. High-resolution inventory of technologies, activities, and emissions of coal-fired power plants in China from 1990 to 2010. Atmos. Chem. Phys. 15, 13299–13317.
Liu, P., Zhang, C., Mu, Y., Liu, C., Xue, C., Ye, C., et al., 2016. The possible contribution of the periodic emissions from farmers' activities in the North China Plain to atmospheric water-soluble ions in Beijing. Atmos. Chem. Phys. 16, 10097–10109.
Liu, P., Zhang, C., Xue, C., Mu, Y., Liu, J., Zhang, Y., et al., 2017c. The contribution of residential coal combustion to atmospheric $PM_{2.5}$ in Northern China during winter. Atmos. Chem. Phys. 17, 11503–11520.
Mason, P.E., Darvell, L.I., Jones, J.M., Williams, A., 2016. Observations on the release of gas-phase potassium during the combustion of single particles of biomass. Fuel 182, 110–117.
Masson, V., 2000. A physically-based scheme for the urban energy budget in atmospheric models. Bound.-Layer Meteorol. 94, 357–397.
McCulloch, A., Aucott, M.L., Benkovitz, C.M., Graedel, T.E., Kleiman, G., Midgley, P.M., et al., 1999. Global emissions of hydrogen chloride and chloromethane from coal combustion, incineration and industrial activities: Reactive chlorine emissions inventory. J. Geophys. Res. Atmos. 104, 8391–8403.
Mlawer, E.J., Taubman, S.J., Brown, P.D., Iacono, M.J., Clough, S.A., 1997. Radiative transfer for inhomogeneous atmospheres: RRTM, a validated correlated-k model for the longwave. J. Geophys. Res. Atmos. 102, 16663–16682.
Paatero, P., Tapper, U., 2010. Positive matrix factorization: A non-negative factor model with optimal utilization of error estimates of data values. Environmetrics 5, 111–126.
Park, M.-B., Lee, T.-J., Lee, E.-S., Kim, D.-S., 2019. Enhancing source identification of hourly $PM_{2.5}$ data in seoul based on a dataset segmentation scheme by positive matrix factorization (PMF). Atmos. Pollut. Res. 10, 1042–1059.
Quan, J., Liu, Q., Li, X., Gao, Y., Jia, X., Sheng, J., et al., 2015. Effect of heterogeneous aqueous reactions on the secondary formation of inorganic aerosols during haze events. Atmos. Environ. 122, 306–312.
Reff, A., Eberly, S.I., Bhave, P.V., 2012. Receptor modeling of ambient particulate matter data using positive matrix factorization: Review of existing methods. J. Air Waste Manage. Assoc. 57, 146–154.
Sheehan, P., Cheng, E., English, A., Sun, F., 2014. China's response to the air pollution shock. Nat. Clim. Change 4, 306–309.
Sun, Y., Du, W., Fu, P., Wang, Q., Li, J., Ge, X., et al., 2016. Primary and secondary aerosols in Beijing in winter: Sources, variations and processes. Atmos. Chem. Phys. 16, 8309–8329.
Sun, Y., Jiang, Q., Wang, Z., Fu, P., Li, J., Yang, T., et al., 2014. Investigation of the sources and evolution processes of severe haze pollution in Beijing in January 2013. J. Geophys. Res. Atmos. 119, 4380–4398.
Sun, Y., Zhuang, G., Wang, Y., Han, L., Guo, J., Dan, M., et al., 2004. The air-borne particulate pollution in Beijing—concentration, composition, distribution and sources. Atmos. Environ. 38, 5991–6004.
Tao, J., Zhang, Z., Tan, H., Zhang, L., Wu, Y., Sun, J., et al., 2018. Observational evidence of cloud processes contributing to daytime elevated nitrate in an urban atmosphere. Atmos. Environ. 186, 209–215.
Thompson, G., Field, P.R., Rasmussen, R.M., Hall, W.D., 2008. Explicit forecasts of winter precipitation using an improved bulk microphysics scheme. Part ii: Implementation of a new snow parameterization. Mon. Weather Rev. 136, 5095–5115.
Thurston, G.D., Ito, K., Lall, R., 2011. A source apportionment of U.S. fine particulate matter air pollution. Atmos. Environ. 45, 3924–3936.
Tian, M., Liu, Y., Yang, F., Zhang, L., Peng, C., Chen, Y., et al., 2019. Increasing importance of nitrate formation for heavy aerosol pollution in two megacities in Sichuan Basin, Southwest China. Environ. Pollut. 250, 898–905.
Wang, G., Zhang, R., Gomez, M.E., Yang, L., Levy Zamora, M., Hu, M., et al., 2016a. Persistent sulfate formation from London fog to Chinese haze. Proc. Natl. Acad. Sci. USA 113, 13630–13635.
Wang, J., Zhou, M., Liu, B.S., Wu, J.H., Peng, X., Zhang, Y.F., et al., 2016b. Characterization and source apportionment of size-segregated atmospheric particulate matter collected at ground level and from the urban canopy in Tianjin. Environ. Pollut. 219, 982–992.
Wang, S., Nan, J., Shi, C., Fu, Q., Gao, S., Wang, D., et al., 2015. Atmospheric ammonia and its impacts on regional air quality over the megacity of Shanghai, China. Sci. Rep. 5, 15842.
Wang, Y., Jia, C., Tao, J., Zhang, L., Liang, X., Ma, J., et al., 2016c. Chemical characterization and source apportionment of $PM_{2.5}$ in a semi-arid and petrochemical-industrialized city, Northwest China. Sci. Total. Environ. 573, 1031–1040.
Watson, J.G., 2011. Visibility: Science and regulation. J. Air Waste Manage. Assoc. 52, 628–713.
Weijers, E.P., Khlystov, A., Brink, H.M.t., 2000. Teom performance when sampling pure ammonium nitrate aerosol. J. Aerosol Sci. 31, 25–26.
Wild, O., Zhu, X., Prather, M.J., 2000. Fast-j: Accurate simulation of in- and below-cloud photolysis in tropospheric chemical models. J. Atmos. Chem. 37, 245–282.
Xie, R., Seip, H.M., Wibetoe, G., Nori, S., McLeod, C.W., 2006. Heavy coal combustion as the dominant source of particulate pollution in Taiyuan, China, corroborated by high concentrations of arsenic and selenium in PM10. Sci. Total. Environ. 370, 409–415.
Ye, C., Liu, P., Ma, Z., Xue, C., Zhang, C., Zhang, Y., et al., 2018. High H_2O_2 concentrations observed during haze periods during the winter in beijing: Importance of H_2O_2 oxidation in sulfate formation. Environ. Sci. Tech. Let. 5, 757–763.
Yu, Y., He, S., Wu, X., Zhang, C., Yao, Y., Liao, H., et al., 2019. PM2.5 elements at an urban site in yangtze river delta, china: High time-resolved measurement and the application in source apportionment. Environ. Pollut. 253, 1089–1099.
Yun, H., Wang, T., Wang, W., Tham, Y.J., Li, Q., Wang, Z., et al., 2018. Nighttime NO_x loss and $ClNO_2$ formation in the residual layer of a polluted region: Insights from field measurements and an iterative box model. Sci. Total. Environ 622-623, 727–734.
Zaveri, R.A., Easter, R.C., Fast, J.D., Peters, L.K., 2008. Model for simulating aerosol interactions and chemistry (MOSAIC). J. Geophys. Res. 113, D13204.
Zaveri, R.A., Peters, L.K., 1999. A new lumped structure photochemical mechanism for large-scale applications. J. Geophys. Res. Atmos. 104, 30387–30415.
Zhang, K., Shang, X., Herrmann, H., Meng, F., Mo, Z., Chen, J., et al., 2019. Approaches for identifying $PM_{2.5}$ source types and source areas at a remote background site of south China in spring. Sci. Total. Environ. 691, 1320–1327.
Zhang, Q., Streets, D.G., Carmichael, G.R., He, K.B., Huo, H., Kannari, A., et al., 2009. Asian emissions in 2006 for the nasa intex-b mission. Atmos. Chem. Phys. Discuss. 9, 5131–5153.
Zhang, R., Wang, G., Guo, S., Zamora, M.L., Ying, Q., Lin, Y., et al., 2015. Formation of urban fine particulate matter. Chem. Rev. 115, 3803–3855.
Zhang, W., Guo, J., Sun, Y., Yuan, H., Zhuang, G., Zhuang, Y., et al., 2007. Source apportionment for urban PM_{10} and $PM_{2.5}$ in the Beijing area. Chin. Sci. Bull. 52, 608–615.
Zhang, Z., Wang, W., Cheng, M., Liu, S., Xu, J., He, Y., et al., 2017. The contribution of residential coal combustion to $PM_{2.5}$ pollution over China's Beijing-Tianjin-Hebei region in winter. Atmos. Environ. 159, 147–161.
Zhao, X.J., Zhao, P.S., Xu, J., Meng, W., Pu, W.W., Dong, F., et al., 2013. Analysis of a winter regional haze event and its formation mechanism in the North China Plain. Atmos. Chem. Phys. 13, 5685–5696.
Zheng, B., Huo, H., Zhang, Q., Yao, Z.L., Wang, X.T., Yang, X.F., et al., 2014. High-resolution mapping of vehicle emissions in China in 2008. Atmos. Chem. Phys. 14, 9787–9805.
Zhou, L., Hopke, P.K., Zhao, W., 2012. Source apportionment of airborne particulate matter for the speciation trends network site in Cleveland. OH. J. Air Waste Manage. Assoc 59, 321–331.
Zíková, N., Wang, Y., Yang, F., Li, X., Tian, M., Hopke, P.K., 2016. On the source contribution to Beijing $PM_{2.5}$ concentrations. Atmos. Environ. 134, 84–95.